ISSN 2635-1676, Nanobiotechnology Reports, 2021, Vol. 16, No. 6, pp. 755–760. © Pleiades Publishing, Ltd., 2021.
Russian Text © The Author(s), 2021, published in Rossiiskie Nanotekhnologii, 2021, Vol. 16, No. 6, pp. 787–792.

NANOELECTRONICS AND NEUROMORPHIC COMPUTER SYSTEMS

Simulation of a Central Pattern Generator Using Memristive Devices

A. A. Suleimanova[a,b,*], M. O. Talanov[a,b], D. N. Masaev[a,b], N. V. Prudnikov[c,d], O. V. Borshchev[e], M. S. Polinskaya[e], M. S. Skorotetskiy[e], S. A. Ponomarenko[e], A. V. Emelyanov[c], V. A. Demin[c], L. A. Feigin[c,f], and V. V. Erokhin[c,g]

[a] *Kazan Federal University, Kazan, 420008 Russia*
[b] *"B-Rain Labs", Kazan, 420111 Russia*
[c] *National Research Centre "Kurchatov Institute", Moscow, 123182 Russia*
[d] *Moscow Institute of Physics and Technology, Dolgoprudnyi, Moscow oblast, 141700 Russia*
[e] *Enikolopov Institute of Synthetic Polymeric Materials, Russian Academy of Sciences, Moscow, 117393 Russia*
[f] *Shubnikov Institute of Crystallography, Federal Scientific Research Centre "Crystallography and Photonics", Russian Academy of Sciences, Moscow, 119333 Russia*
[g] *Institute of Materials for Electronics and Magnetism, National Research Council (IMEM-CNR), Parma, 43124 Italy*
**e-mail: sulemanovaaa@gmail.com*

Received June 25, 2021; revised July 9, 2021; accepted July 19, 2021

Abstract—The central pattern generator (CPG) is one of the key elements of the nervous system of Vertebrates, determining the motor, breathing, swallowing, etc. cyclic motor patterns of a living organism, which require constant maintenance and prompt (or immediate) recovery in the case of injury. In this context, the construction of neuroprosthetic systems requires the development of electronic analogs (the corresponding CPGs). It is proposed to use memristive devices as adaptive elements with continuous tunable characteristics in these systems, because they exhibit a property, similar to bio-synaptic plasticity. The CPG model is developed, which yields an output activity, similar to that of biological objects. The requirements for the temporal characteristics of tunable elements for their successful use as artificial synapses are also specified. Memristive devices of a new type are fabricated according to the Langmuir–Schaefer technique using benzothieno[3,2-*b*] [1]-benzothiophene (BTBT) dimer as an active layer. BTBT-based devices make it possible to switch the conductivity at low voltages and currents, which is important in the development of energy-efficient neuroprosthetic systems, and the characteristic switching times are about several hundred milliseconds, which indicates that they can be used as analogs of synapses upon instrumental realization of the CPG.

DOI: 10.1134/S2635167621060240

INTRODUCTION

The ability of neuromorphic systems to imitate the operation of individual parts of the nervous system and the brain is an important specific feature [1]. It is critical that these systems must be implemented at the device level, because it will allow for parallel data processing and provide energy efficiency, which is especially urgent in the formation of implantable neuroprosthetic devices.

Currently, memristive devices are widely used in the development of neuromorphic systems, because they exhibit some peculiar properties, which make it possible to consider them as electronic analogs of biological synapses [2–9]. These elements have been successfully used to construct networks, capable of Hebbian learning [10–13], and even for the synaptic connection of two living neurons of the cerebral cortex of a rat [14], which can be considered as the first step in developing a synapse prosthesis.

Organic memristive devices are of particular interest because they do not require electroforming (which, as a rule, requires the application of high voltages) and can be organized in a flexible arrangement [15–21]. Both these features are necessary factors in considering the possibility for the formation of implantable systems.

The central pattern generator (CPG) is a vital part of the nervous system, which determines the formation of a sequence of pulses, required for some actions (e.g., the coordinated stimulation and inhibition of muscles during walking, taking into account stimuli, arriving from the tactile sensors of the foot skin) [22]. In this context, it is important to implement a CPG analog using memristive devices.

Currently, the possibility for implementing CPG using memristive devices was considered in two studies. In particular, a circuitry solution for this problem was proposed in [23]. Although the corresponding block diagram was designed and simulation showed its

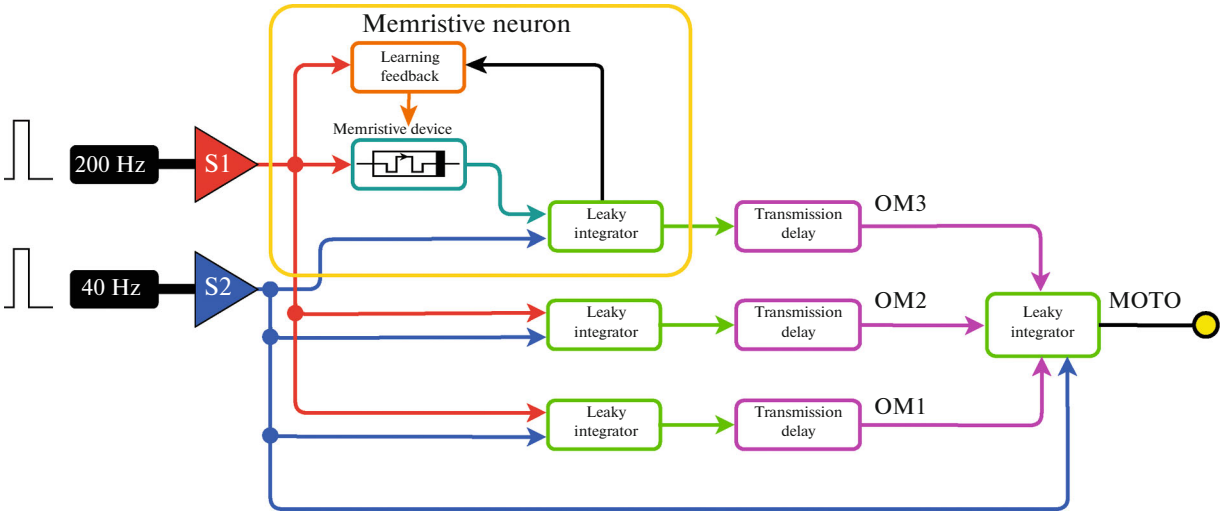

Fig. 1. Simplest scheme of a CPG for connecting the motor neurons of a reflector-arc part and second-level interneurons, which generates the walking pattern. Two signals with frequencies of (*S*1) 200 and (*S*2) 40 Hz, which correspond to the sensor input and epidural stimulation, respectively, are supplied to interneurons (OM1–3), where OM3 is implemented using a memristive neuron. Only the 40-Hz signal is supplied to the motor neuron.

fundamental functionality, the requirements for the element base (in particular, memristive devices), which would guarantee the possibility for its physical implementation, were not formulated. A method, which was assumed to be used for instrumental realization of a half center oscillator (an important CPG element), was proposed in [24]. Not only the simulation data but also experimental results were shown in that study. Among the possible drawbacks of the proposed solution, one can mention the absence of mechanical plasticity of used silicon-based memristive devices, which is preferred upon the implementation of implantable devices.

Successful instrumental realization of a pattern generator consists of the following three stages: development of a block diagram and simulation of its operation (as a result, this stage should yield requirements for the properties of memristive devices); the implementation and testing of memristive devices with the required properties; and the fabrication and testing of an analog of a pattern generator.

The purpose of this study is to realize the first two stages of the proposed scenario: development and testing of a block diagram and implementation of the necessary memristive devices with the required properties. The memristive devices are fabricated using benzothieno[3,2-*b*] [1]-benzothiophene (BTBT). This compound is chosen for active-channel realization due to the following two factors. First, recently, derivative compounds of benzothiophene have been of significant interest due to a high carrier mobility (up to 1 $cm^2/V\,s$) [25]. The siloxane dimer of BTBT makes it possible to form a two-dimensional crystalline single layer according to the Langmuir technique due to hydrogen bonds between the siloxane group and water molecules. Long aliphatic spacers increase the solubility in organic solvents, which makes it possible to prepare films using different methods. Second, this compound was not previously used for the formation of memristive devices.

EXPERIMENTAL

Simulation

Figure 1 shows a block diagram of the CPG and high-level description of the experiment, where a motor neuron is subjected to epidural electrical stimulation (EES) at a frequency of 40 Hz (the most efficient frequency for neurorehabilitation [26, 27]). The CPG consists of two levels: the monosynaptic level, in which afferents (sensor neurons) affect directly the motor neuron, which passes the signal to the muscle, and the polysynaptic level, which processes the input signals from the afferents and passes them to the motor neuron indirectly via interneurons of the spinal cord (OM1–3). In this diagram, the monosynaptic level is approximated by a 40 Hz generator (EES) and the soma of a motor-neuron cell (implemented as leaky integrator MOTO). The polysynaptic-level interneurons are activated by a coactivation of a sensor input signal with a frequency of 200 Hz and a EES with a frequency of 40 Hz. The CPG consists of three levels (OM1–3), where OM3 is implemented using a memristive neuron. As a result, a monosynaptic response to 40 Hz stimulation and a polysynaptic response to the interneuron stimulation are formed on the motor neuron.

The schematic diagram of the memristive neuron (shown by the rectangle in Fig. 1) consists of the following parts: input signals, a memristive device, a

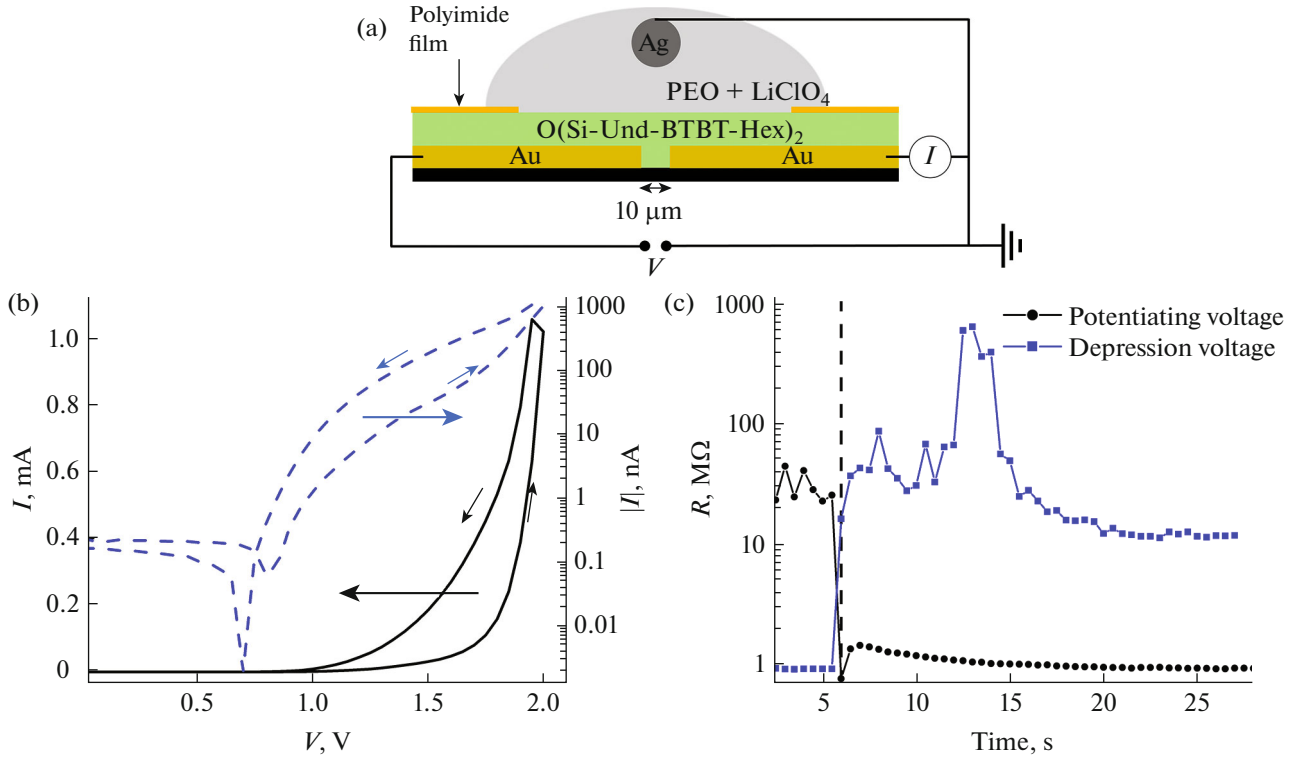

Fig. 2. (a) Structure and power-supply circuit of the memristive device. (b) Cyclic current–voltage characteristics of the fabricated device in (on the left) conventional and (on the right) logarithmic coordinates. Direction of the curve traversal is indicated by the arrows. (c) Kinetics of switching to the conducting and nonconducting states.

leaky integrator, and learning feedback. Triangles *S*1 and *S*2 are input excitation channels (200 and 40 Hz) for receiving positive spike signals (neuron potentials) to the artificial neuron scheme. When signal *S*1 passes through the memristive device, its amplitude changes depending on the memristor resistance. The following part of the CPG electric circuit, which plays the role of a soma (cell body) of a biological neuron in the developed artificial neuron, is a leaky integrator, which consists of a RC chain for charging and discharging the electric potential; an integrator of the signals, passed through the RC circuit; and a threshold, at which the output signal is formed. The generated output signal is transferred, first, to the excitation inputs of other neurons, passing through the transmission-delay block, and, second, to the learning feedback, where (along with signal *S*1) it forms time delay Δt. The transmission-delay chain simulates/implements the time of signal transmission over a biological-neuron axon and in a synapse between neurons and is a part of the RC chain, designed to form a time delay of the input signal, which depends on the capacitance (it increases from OM1 to OM3) of the capacitor, located in this circuit. The learning feedback generates pulses, which depend on Δt and change the memristor resistance. Based on the formed delay Δt between the input and output signals of the memristive neuron, the learning feedback generates pulses in the spike-timing dependent plasticity (STDP) form of Hebbian learning, which increase or decrease the memristor conductivity. The schematic diagram was simulated using the LTSpice software package.

Fabrication of a Memristive Device

The material was synthesized according to the technique described in [28]. The compound was dissolved in toluene in a concentration of 0.33 g/L. The Langmuir layers were formed in a Minitrough (KSV, Finland) with a maximum area of 243 cm^2 under compression at a rate of 7.5 cm^2/min to a pressure of 30 mN/m. After compression, 10 layers were successively transported in the horizontal direction. The substrates were SiO_2 on Si wafers with gold electrodes on a chromium sublayer, fabricated using explosive photolithography. The interelectrode distance was 10 μm.

After film formation and drying, a small portion around the channel was limited by a polyimide film. Then, a polymer electrolyte was deposited, which consisted of polyethylene oxide (PEO, 600 000 g/mol) with a concentration of 75 g/L and perchlorate lithium with a concentration of 0.65 M in acetonitrile. A silver wire 50 μm in diameter, used as a counter electrode, was placed into the electrolyte. After all operations, the device was dried in an air flow for 2 h. The device structure and power-supply circuit are shown in Fig. 2a.

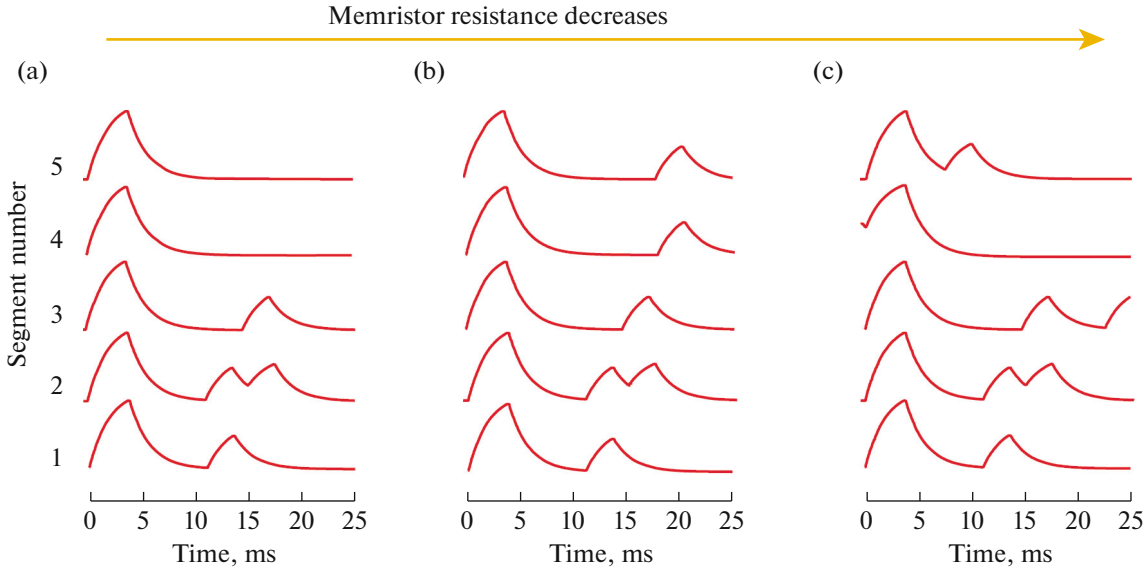

Fig. 3. Recording of the potential of the 125-ms-long motor neuron, sliced into five 25-ms-long segments in correspondence with a stimulation frequency of 40 Hz, using the LTSpice simulator (monosynaptic and polysynaptic responses are in the ranges of 0–5 and 10–25 ms, respectively). (a) High memristor resistance: polysynaptic responses on slices 4 and 5 are absent. (b) Medium memristor resistance: polysynaptic responses are formed in the range of 18–25 ms. (c) Low memristor resistance: polysynaptic responses are formed randomly on slices 3–5.

RESULTS AND DISCUSSION

Figure 2b shows the typical cyclic current–voltage characteristic of the fabricated device in conventional (solid curve) and logarithmic (dotted curve) coordinates. In the experiment, the voltage step was 50 mV and the hold time of each voltage value was 1 s. It can be seen in Fig. 1 that the fabricated memristive element yields different currents in the forward and backward directions of the voltage change in the range from 1.2 to 1.6 V, which is indicative of the presence of resistive switching in the material under study. The possible reasons for this switching in these structures are the formation of a double electrical layer [30]; doping with protons, formed from trace amounts of water [31]; and the electrochemical redox reaction [32]. Detailed analysis of the switching mechanisms requires additional investigations and is beyond the scope of this study.

Figure 2c shows a change in the device resistance at potentiating (+2 V) and depressing (–0.1 V) voltages. The switch-on instants of the corresponding voltages are indicated by vertical dotted lines. The sampling rate was 0.5 s. Even for the first measurement after switching on the voltage, the device resistance changed radically. This means that the characteristic time of a change in the conductivity of this device is several hundred milliseconds.

A structure with three interneuron levels (OM), which was modelled using LTSpice, is shown in Fig. 1a. Two signals with frequencies of 40 and 200 Hz were supplied to each OM (the 200-Hz signal was switched successively from OM1 to OM3, which corresponded to a change in the sensor input upon heel-to-toe weight transfer). The output signal from OM was transferred with a delay to a motor neuron, the value of which increased successively from OM1 to OM3. At the supply of a 200-Hz signal to OM3, its resistance was varied to simulate the operation of a memristor (the results are shown in Fig. 3). The plots show the potential of a 125-ms-long motor neuron, sliced into five segments with lengths of 25 ms in correspondence with the 40-Hz stimulus, where the monosynaptic response is in the range from 0 to 5 ms and stronger than the polysynaptic response. The first segments (1, 2) are not changed, because the polysynaptic responses are caused by OM1 and OM2 (the resistance at the input of these levels was not varied). In the first case (Fig. 3a), the memristor resistance is high (100 MΩ) and polysynaptic responses are not formed on segments 4 and 5, because the amplitude of the 200-Hz signal at the OM3 input after transmission through the memristor is insufficient (upon summation with the 40 Hz signal) to exceed the threshold at the leaky integrator. The required walking pattern (Fig. 3b), similar to the biological one [29], is formed at the medium memristor resistance (25 MΩ), because the output signal of the memristive neuron is formed in the case of summation of two signals from the 200-Hz and 40-Hz generators. In the third case, at a low resistance of 1 MΩ (Fig. 3c), the polysynaptic responses are formed randomly (at the end of slice 3, at the beginning of slice 4, and on slice 5 immediately

after the monosynaptic response), which does not facilitate walking-pattern formation. This situation occurs because one 200-Hz stimulus applied to the memristive neuron is sufficient for output-signal formation.

Thus, the hypothesis of the applicability of memristive devices, the difference in the resistances of which at the ON and OFF states is two orders of magnitude, was proposed and simulated. There exists the optimal value of the memristive-device resistance for formation of the correct walking pattern in a CPG.

CONCLUSIONS

The simplest scheme of a central pattern generator was proposed. This scheme was simulated in LTSpice and consisted of three analog interneurons (one of which is memristive) and one motor neuron. The performed CPG simulation made it possible to determine the optimal weights (memristor resistances), sufficient for the formation of interneuron responses, which will be implemented in an instrumental device. A memristive device, which completely corresponded to the requirements, established at the simulation stage, was also fabricated and investigated. We note that the compound, which was used for the active channel of the device, was used for the first time in the implementation of memristive devices. Further studies will be aimed at the physical implementation and testing of a pattern generator, based on the developed memristive devices. We hope that these studies bring closer the prospect of forming adaptive neuromorphic systems, which are used for neural prostheses of the most important motor functions of an organism.

ACKNOWLEDGMENTS

We are grateful to Yu.N. Malakhova for the help in fabricating the memristive elements.

FUNDING

This study was supported by the Russian Foundation for Basic Research, project no. 19-29-03057.

REFERENCES

1. V. Erokhin, BioNanoSci. **10**, 834 (2020). https://doi.org/10.1007/s12668-020-00795-1
2. T. Chang, S.-H. Jo, K.-H. Kim, et al., Appl. Phys. A **102**, 857 (2011). https://doi.org/10.1007/s00339-011-6296-1
3. V. Erokhin, T. Berzina, P. Camorani, et al., BioNanoSci. **1** (1), 24 (2011). https://doi.org/10.1007/s12668-011-0004-7
4. G. Indiveri, B. Linares-Barranco, R. Legenstein, et al., Nanotechnology **24**, 384010 (2013). . https://doi.org/10.1088/0957-4484/24/38/384010
5. B. Gao, Y. Bi, H.-Y. Chen, et al., ACS Nano **8**, 6998 (2014). https://doi.org/10.1021/nn501824r
6. S. la Barbera, D. Vuillaume, and F. Alibart, ACS Nano **9**, 941 (2015). https://doi.org/10.1021/nn506735m
7. W. Banerjee, Q. Liu, H. Lv, et al., Nanoscale **9**, 14442 (2017). . https://doi.org/10.1039/c7nr04741j
8. A. S. Sokolov, M. Ali, R. Riaz, et al., Adv. Funct. Mater. **29**, 1807504 (2019). https://doi.org/10.1002/adfm.201807504
9. B. Tian, L. Liu, M. Yan, et al., Adv. Electron. Mater. **5**, 1800600 (2019). https://doi.org/10.1002/aelm.201800600
10. K. D. Cantley, A. Subramaniam, H. J. Stiegler, et al., IEEE Trans. Nanotechnol. **10**, 1066 (2011). https://doi.org/10.1109/TNANO.2011.2105887
11. T. Serrano-Gotarredona, T. Masquelier, T. Prodromakis, et al., Front. Neurosci. **7**, 2 (2013). https://doi.org/10.3389/fnins.2013.00002
12. K. E. Nikiruy, A. V. Emelyanov, V. A. Demin, et al., AIP Adv. **9**, 065116 (2019). https://doi.org/10.1063/1.5111083
13. N. Prudnikov, D. Lapkin, A. V. Emelyanov, et al., J. Phys. Appl. Phys. **53**, 414001 (2020). https://doi.org/10.1088/1361-6463/ab9262
14. E. Juzekaeva, A. Nasretdinov, S. Battistoni, et al., Adv. Mater. Technol. **4**, 1800350 (2018). https://doi.org/10.1002/admt.201800350
15. M. P. Fontana and V. Erokhin, J. Comput. Theor. Nanosci. **8**, 313 (2011). https://doi.org/10.1166/jctn.2011.1695
16. S. Kim, H. Y. Jeong, S. K. Kim, et al., Nano Lett. **11**, 5438 (2011). . https://doi.org/10.1021/nl203206h
17. N. Raeis-Hosseini and J.-S. Lee, ACS Appl. Mater. Interfaces **8**, 7326 (2016). https://doi.org/10.1021/acsami.6b01559
18. Y. Cai, J. Tan, L. YeFan, et al., Nanotechnology **27**, 275206 (2016). https://doi.org/10.1088/0957-4484/27/27/275206
19. Q. Chen, M. Lin, Z. Wang, et al., Adv. Electron. Mater. **5**, 1800852 (2019). https://doi.org/10.1002/aelm.201800852
20. S. Battistoni, C. Peruzzi, A. Verna, et al., Flex. Print. Electron. **4**, 044002 (2019). https://doi.org/10.1088/2058-8585/ab4dce
21. B. S. Shvetsov, A. N. Matsukatova, A. A. Minnekhanov, A. A. Nesmelov, B. V. Goncharov, D. A. Lapkin, M. N. Martyshov, P. A. Forsh, V. V. Rylkov, V. A. Demin, and A. V. Emelyanov, Tech. Phys. Lett. **45**, 1103 (2019). https://doi.org/10.1134/S1063785019110130
22. S. Grillner, Nat. Rev. Neurosci. **4**, 573 (2003). https://doi.org/10.1038/nrn1137

23. I. Köymen and E. M. Drakakis, Int. J. Circuit Theory Appl. **46**, 1294 (2018). https://doi.org/10.1002/cta.2487

24. R. Midya, Z. Wang, S. Asapu, et al., Adv. Electron. Mater. **5**, 1900060 (2019). https://doi.org/10.1002/aelm.201900060

25. I. Temiño, F. G. D. Pozo, M. R. Ajayakumar, et al., Adv. Mater. Technol. **1**, 1600090 (2016). https://doi.org/10.1002/admt.201600090

26. I. Lavrov, C. J. Dy, A. J. Fong, et al., J. Neurosci. **28**, 6022 (2008). https://doi.org/10.1523/JNEUROSCI.0080-08.2008

27. Y. P. Gerasimenko, I. A. Lavrov, G. Courtine, et al., J. Neurosci. Methods. **157**, 253 (2006). https://doi.org/10.1016/j.jneumeth.2006.05.004

28. O. Borshchev, A. Sizov, E. Agina, et al., Chem. Commun. **53**, 885 (2016). https://doi.org/10.1039/C6CC08654C

29. P. Gad, I. Lavrov, P. Shah, et al., J. Neurophysiol. **110**, 1311 (2013). https://doi.org/10.1152/jn.00169.2013

30. P. A. Shaposhnik, S. A. Zapunidi, M. V. Shestakov, et al., Russ. Chem. Rev. **89**, 1483 (2020). https://doi.org/10.1070/RCR4973

31. B. C. Das, B. Szeto, D. D. James, et al., J. Electrochem. Soc. **161** (12), H831 (2014). https://doi.org/10.1149/2.0831412jes

32. D. Lapkin, A. Emelyanov, V. Demin, et al., Appl. Phys. Lett. **112**, 043302 (2018). https://doi.org/10.1063/1.5013929

Translated by A. Sin'kov